Leckie, R.M., Sigurdsson, H., Acton, G.D., and Draper, G. (Eds.), 2000
Proceedings of the Ocean Drilling Program, Scientific Results, Vol. 165

14. MICROBIAL ORIGIN OF MICROCRYSTALLINE CARBONATE SEDIMENT AND CEMENTS FILLING FRACTURES IN BASALTS RECOVERED AT SITE 1001, CARIBBEAN SEA[1]

Maria Mutti[2]

ABSTRACT

This paper presents the results of a petrographic and scanning electron microscope study of carbonate sediments and cements found within basalts cored at Ocean Drilling Program Site 1001. The basaltic sequence is pervasively cut by fractures that show vugs filled by carbonate cements. This study focuses on the nature of micritic sediment and cements and documents the occurrence of two types of micrites. The first (m1) has been observed at only one location (interval 165-1001A-54R-5, 13–18 cm). It consists of recrystallized pelagic carbonate, which was infiltered from the seafloor and deposited within the newly formed cavities within the basalt. The second micrite (m2) is more widespread and is present as an asymmetrical, mostly geopetal lining of fractures and cavities. Optical microscopy reveals laminae characterized by undulated upper surfaces that contain micritic lumps forming pseudopeloids. Typically, these structures are considered to result from the dismantling of microbial filamentous mats.

The data generated in this study present evidence for a new mechanism for the origin of micrite that is commonly found within basalt sequences. Results from previous studies indicate this cement is formed in situ, but the new data indicate precipitation is controlled by processes related to microbial activity. At this stage of study, additional data are needed to determine whether this precipitation process takes place in marine or marine-modified pore waters.

INTRODUCTION

Site 1001 of Ocean Drilling Program (ODP) Leg 165 was drilled in the Caribbean Sea on the Hess Escarpment of the lower Nicaragua Rise (Fig. 1) where Neogene sediments are thin and a continuous Cretaceous–Paleogene sedimentary section overlying basaltic basement could be recovered. One of the objectives at this site was to recover igneous basement and test models for the formation of the Caribbean Oceanic Plateau. The top of the basaltic sequence at Site 1001 was encountered at a depth of 485.4 meters below seafloor (mbsf) at a water depth of 3259.6 m. A 37.65-m-thick section of basaltic rocks, primarily of extrusive origin, was drilled in Hole 1001A. The basalts are overlain by Campanian age limestones and clayey limestones containing nannofossils that indicate a minimum age of 77 Ma (Sigurdsson, Leckie, Acton, et al., 1997).

The basaltic sequence in Hole 1001A was divided shipboard into 12 units (Units A through L), which represent individual lava flows and associated hyaloclastite breccias (Sigurdsson, Leckie, Acton, et al., 1997) (Fig. 2). Sinton et al. (Chap. 15, this volume) describe the petrology of the basalts and discuss their geochronology. These basalts are interpreted to represent sheet flows associated with volcanic events of high mass eruption rates (Sigurdsson, Leckie, Acton, et al., 1997). The hyaloclastite breccias on top of these flows, which are the boundary between the sheet flow and seawater, are expected to have been an area of vigorous thermal convection where the transfer of heat out of the lava may result in extensive mineralization.

The basaltic sequence is characterized by a pervasive system of carbonate-cement–filled fractures and vugs, which are particularly well developed in Core 165-1001A-54R (Fig. 2). Studies of secondary carbonate minerals found in oceanic basalts at Deep Sea Drilling Project and ODP sites provide constraints on the relative timing of carbonate mineral precipitation. Low-temperature (generally <80°C) basalt alteration in seawater takes place in three stages: (1) palagonite formation, (2) smectite formation, and (3) carbonate mineral formation (Boehlke et al., 1980; Staudigel et al., 1986).

Macroscopic observations on the samples recovered from Hole 1001A reveal that the stage of "carbonate mineral formation" in reality contains a variety of generations of carbonate internal sediments and cements characterized by complex paragenetic sequences. The purpose of this article is to describe the textures and the relative timing of occurrence of the carbonate internal sediments and cements deposited within the basalt sequence with particular focus on the origin of the internal sediment. Micritic internal sediment has often been described with geopetal textures within basalt sequences (Bernoulli et al., 1978) and ophicalcites (Folk and McBride, 1976; Bernoulli and Weissert, 1985), but its origin has remained controversial. Folk and McBride (1976), on the basis of spatial distribution, increasing abundance toward topographic highs, and the resemblance of features to caliche soils, have suggested a pedogenic origin for the micrite found in ophicalcites from the Italian Apennines. Bernoulli et al. (1978) recognized four different generations of carbonate internal sediment all of marine origin within Miocene basalts from Hole 373A, in the Tyrrhenian Basin. More specifically, they identified both an internal sediment derived from pelagic oozes and a diagenetic sediment precipitated and redeposited within the cavities in the presence of seawater.

METHODS

The basalt cores containing fractures and vugs filled by carbonate phases were investigated macroscopically. The macroscopic observations on the core surface revealed a variety of carbonate internal sediments and cements characterized by complex paragenetic sequences. This study focuses on the origin of micritic sediment. Selected samples of representative textures were then chosen, slabbed, and made into thin sections for petrographic analyses. Samples for scanning electron microscope (SEM) study were broken from the thin-section chips and were not subject to selective dissolution.

[1]Leckie, R.M., Sigurdsson, H., Acton, G.D., and Draper, G. (Eds.), 2000. *Proc. ODP, Sci. Results,* 165: College Station, TX (Ocean Drilling Program).
[2]Earth Sciences Department, University of Southern California, Los Angeles, CA 90089-0740, U.S.A. mmutti@earth.usc.edu

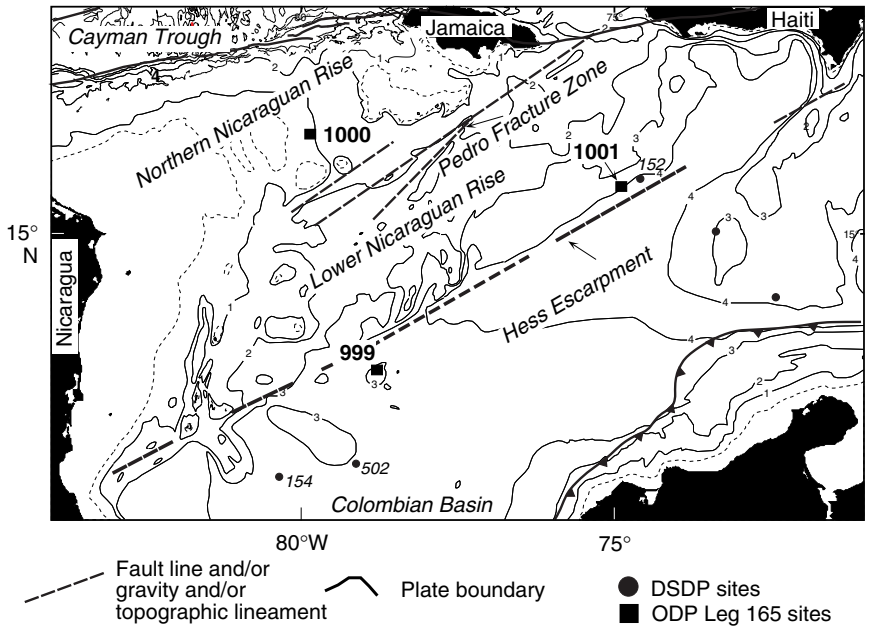

Figure 1. General map of the Western Caribbean. The Colombian Basin and the Nicaraguan Rise are clearly separated by the Hess Escarpment. ODP Site 1001 is the location of this study.

PARAGENESIS OF FRACTURE- AND CAVITY-FILLING CARBONATE SEDIMENTS AND CEMENTS

The distribution of the different carbonate phases at a microscopic scale varies greatly from sample to sample and also within the same thin section. Although a detailed study of these features was beyond the purpose of this paper, the main phases of fracture and cavity filling by carbonate minerals are briefly described here with the purpose of better constraining the timing of formation of the micritic internal sediment and cement relative to basalt alteration and later phases of calcite precipitation. They are discussed in order of paragenesis (Fig. 3).

1. The first phases included initiation of fractures and alteration of basalts. Basalts in contact with the sediment preserve quenched margins with remnant spherulitic structures. Glasses in the contact zone have been completely altered to palagonite and/or smectite. Macroscopic observations indicate that fracturing events happened at different times, as evidenced by crosscutting and superposition of different generations of carbonate cements (Fig. 3). New fractures formed and continued to expand and propagate throughout the paragenetic sequence; they are postdated by progressively younger generations of carbonate cements (Fig. 4).
2. Pelagic internal sediment (micrite 1 [m1]) was infiltrated either during or immediately after the emplacement of the basalts (Fig. 4A). This is suggested by the presence of Campanian carbonate beds that are interbedded between Units E and F, which contain a large number of thick-walled benthic foraminifers typical of upper bathyal environments of the Late Cretaceous (see Sigurdsson, Leckie, Acton, et al., 1997).
3. The basalt was fractured, and fractures were filled by equant sparry calcite ("sparry calcite 1"), which occurs as the first phase of carbonate lining the fracture walls (Fig. 5D). This cement is rare and was observed in only a few samples. Crystals are typically 20–30 µm in size and are inclusion rich (Fig. 5D). This phase is nonsymmetrical in fractures and forms preferentially on the downward side of the fractures.
4. Further fracturing took place with subsequent precipitation/deposition of laminated internal sediments (micrite 2 [m2]) either as the first phase at the base of cavities (discussed in detail below) clearly postdating the alteration of basalts in seawater, or as a second phase in the older fractures containing equant sparry calcite as the first precipitate (Fig. 5A–D).
5. Finally, precipitation of different phases of sparry calcite cements, all referred to for simplicity purposes as "sparry calcite 2," took place. This cement postdates all previous generations and is the latest phase of cavity filling (Fig. 5A–D).

MICRITIC INTERNAL SEDIMENT/CEMENT

On the basis of the textural relationships and petrographic characteristics, two types of micrite have been distinguished: micrite 1 and micrite 2. Micrites, as defined by Folk (1962), are characterized by grains smaller than 4 µm, whereas microspar ranges from 4 to 31 µm in size. Because these grain-size classes may not be clearly divided, some authors use the term to include both micrite and microspar, as I do in this paper.

Micrite 1

This micrite is the first type of carbonate material observed in the basalt sequence and was found only in interval 165-1001A-54R-5, 13–18 cm. It appears to have been infiltered and deposited from the seafloor into the newly formed cavities within the basalts. Physical sedimentation of micrite as laminated and graded deposits took place either during or soon after the last episodes of basalt formation (Fig. 4A). Because of the lack of orientation of the rock fragments containing this phase, it is not possible to assess whether this sediment had geopetal orientation or not. The micrite consists of grains 5–15 µm in size (Fig. 6A, B). Microfossils are not clearly observable in thin section within the micrite, but ghosts of recrystallized nannoplankton can be seen under the SEM (see Fig. 6B), suggesting this sediment has a pelagic origin and consists of nannoplankton ooze. The fact that the sediment is now primarily characterized by grains larger than 5 µm may be explained by recrystallization. Microsparites (see definition above) can be formed by hydrothermal alteration of pelagic ooze (e.g., Easton et al., 1982; in the Indian Ocean). Hydrothermal alteration and overprint has always been considered a reason for why it is difficult to distinguish between recrystallized pelagic and diagenetic

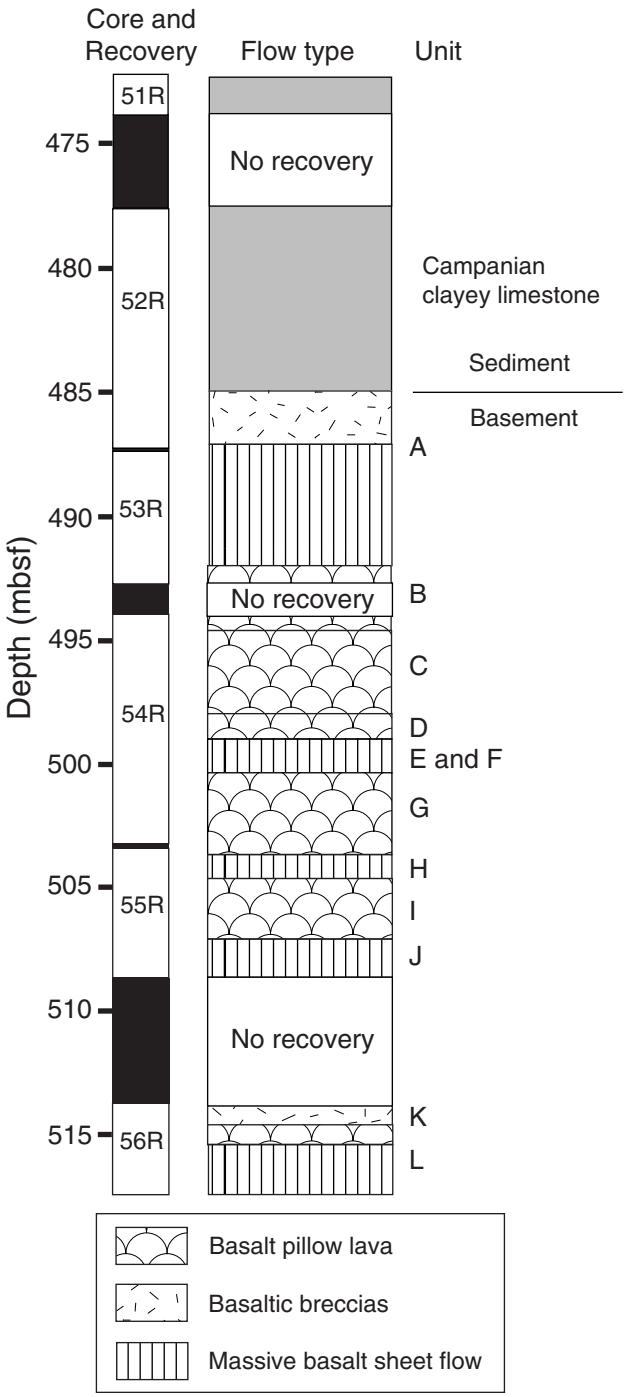

Figure 2. The Cretaceous basaltic basement succession in Hole 1001A included 12 units (Units A through L), consisting dominantly of two flow types: pillow lavas and more massive sheet flows with hyaloclastite breccia at their tops. Column on left indicates core recovery (intervals of no recovery are in black).

internal sediment (cf. Bernoulli et al., 1978; Bernoulli and Weissert, 1985).

In summary, the characteristics of this micritic sediment suggest that it has a pelagic origin and was infiltered down from the seafloor into available pore space. Its deposition took place either between episodes of basalt formation or immediately afterward at an early stage, indicating connection of the pore space with the seafloor.

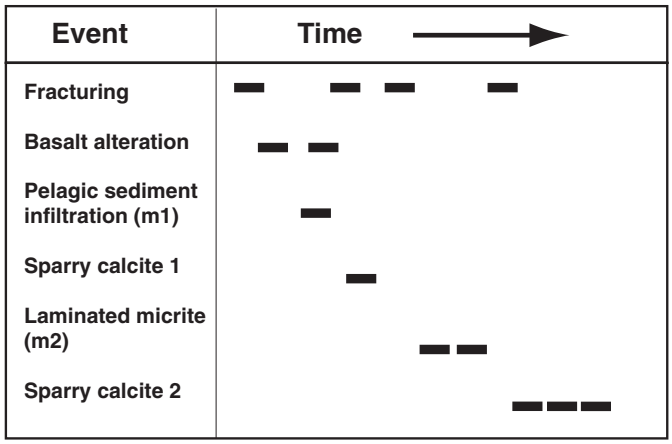

Figure 3. Paragenesis of cavity fills.

Micrite 2

The second type of micrite constitutes an important phase of infilling of the fractures and cavities by carbonate and is particularly well developed throughout Core 165-1001A-54R (Fig. 4B, C). Micrite 2 forms with a geopetal orientation within the horizontal fractures and shows some thickness variation at the millimeter scale (Figs. 4C, 5A, 5C). Within subvertical fractures, micrite 2 forms in an asymmetrical fashion on the downward side of the fracture wall (Figs. 4B, 5C, 5D). Textural relationships indicate that this phase was lithified before further reopening of the fractures and precipitation of the later phases of infilling. In fact, the micrite forms coatings on the fracture wall with a texture that would not be gravitationally stable unless it were lithified. Clearly, infiltration cannot explain the observed textures, and the micrite must have been generated as a cement by in situ precipitation. Under the optical microscope, the micrite shows a laminated structure (Fig. 5A). Laminae are characterized by undulating upper surfaces, which appear to mantle pre-existing topography, and contain micritic lumps of distinctively homogenous grain size (6–10 μm in size) for each lamina (Figs. 5A, 5B, 6C). No evidence is observed for redeposition, such as grading of grains, or evidence for dissolution and reprecipitation at the scale of the laminae. Within the laminae, the micrite are in lumps forming pseudopeloids that appear to be almost "floating" in the later calcite (Fig. 5B). Typically, these types of structures are considered to result from the dismantling of microbial filamentous mats (Monty, 1995). At the SEM scale, the micrite crystals are euhedral to anhedral, and crystal surfaces reveal the presence of small spherules (<1 μm in size), which impart a blobby appearance to the crystals. These spherules are caused by the presence of fossilized bacteria entombed in the micritic calcite crystals (Fig. 6D–H), supporting a microbial origin for micrite 2 (Morita, 1980; Novitski, 1981). In addition, calcified "bridges" exist between grains (Fig. 6E– F), which point to the former presence of bacteria. These crystals, unlike micrite 1, do not show any evidence of recrystallization.

ORIGIN OF THE MICROBIAL MICRITE (MICRITE 2)

Bacteria may play an important role in the precipitation of carbonates, as the consequence of their metabolic activity which alters the physicochemical environment toward increased alkalinity (Monty, 1995). Several mechanisms exist to explain the occurrence of micrite in sedimentary environments, either aerobic or anaerobic, and micrite particles might be generated in-situ by chemical and microbiological precipitation (Monty, 1995). One of these involves the presence of

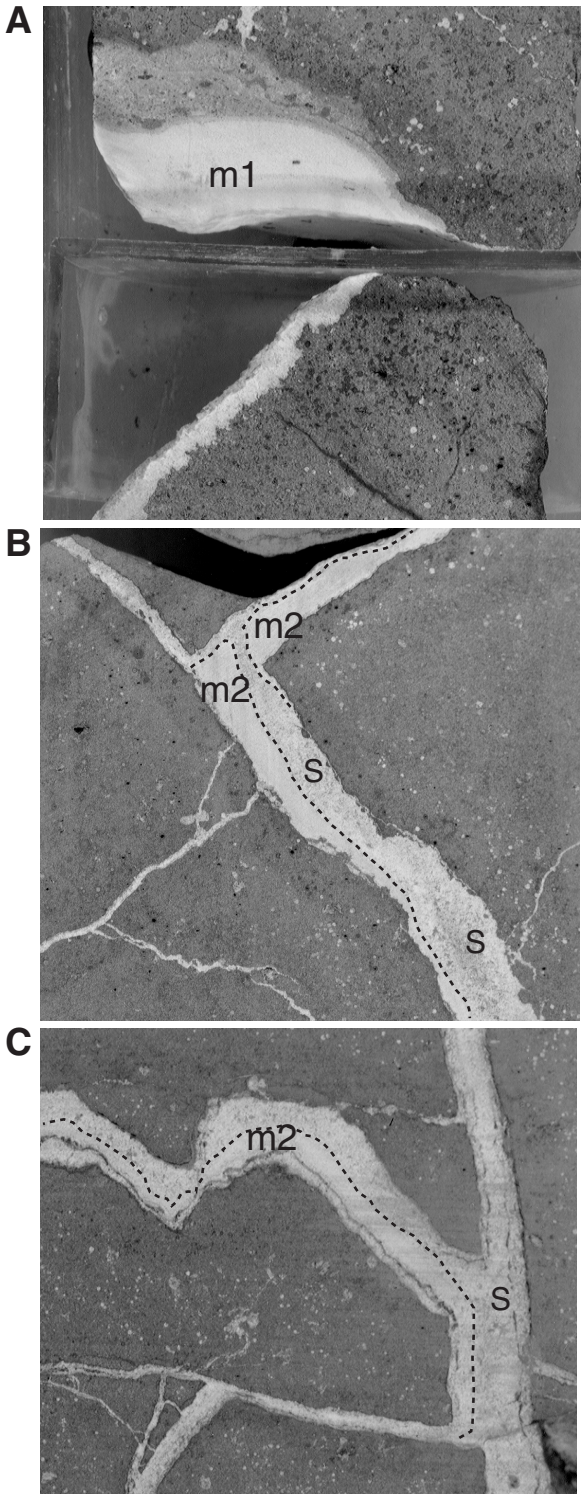

Figure 4. Macroscopic fracture-filling carbonate phases. **A.** Lens of fine-grained carbonate sediment, micrite 1 (m1), composed of recrystallized calcite most likely derived from nannoplankton fragments. The orientation of the sample is not preserved, but it is likely that this was deposited gravitationally at the bottom of the cavity (interval 165-1001A-54R-5, 13–18 cm). **B.** Fracture filled by micrite 2 (m2) and sparry calcite (s). Note the upper boundary of micrite 2, which suggests that lithification took place before further enlargement of the fracture and precipitation of sparry calcite 2 (s) (interval 165-1001A-54R-2, 63–68 cm). **C.** Fracture partially filled by micrite 2 with a geopetal orientation at the lower side of the fracture, and later by sparry calcite (s) (interval 165-1001A-54R-2, 51.5–55 cm).

microbial mats, consisting of a "constructional" community of bacteria, along with bacteria involved in the degradation of these organisms (Chafetz and Buczynski, 1992). The occasional occurrence of iron oxides lining the cavity walls suggests that the environment in which micrite 2 precipitated was oxic. Microbes that could survive under these cavity-dwelling conditions possibly relied on a complex heterotrophic or chemotrophic system.

CONCLUSIONS

This study has identified a paragenetic sequence of the major phases of carbonate deposition forming in fractures and cavities within the basalts recovered at Site 1001 and their infilling by carbonate sediment and cements. More specifically, two types of micrite (micrite 1 and micrite 2) have been identified on the basis of textural characteristics, optical microscopy, and SEM petrography. The first type, micrite 1, is a pelagic sediment infiltered from above seafloor and deposited either during or immediately after the emplacement of the basalt sequences. The second type, micrite 2, clearly postdates the formation of the breccias and the alteration of the basalt in seawater and has been generated by precipitation in situ. Its irregularly laminated character suggests that it is the product of dismantling of microbial filamentous mats. SEM images reveal the traces of fossilized bacteria entombed in the micritic calcite crystals that generate blobby crystal surfaces.

The petrographic data presented in this paper indicate that micrite 1 was recrystallized, whereas micrite 2 was not. This suggests that the formation of micrite 2 postdated the major phase of hyrdothermal alteration of the basalts. On the basis of this observation, we can exclude the hypothesis that all the calcite is of hydrothermal origin. This would imply that the lavas had a rapid cooling history and lost their heat to the ocean without any significant precipitation in the voids.

More generally, the data of this study present evidence for a new mechanism for the origin of micrite, which is commonly found within basalt sequences. In accordance with results from previous studies (e.g., Bernoulli and Weissert, 1985) this cement is formed in situ, but what is new is that precipitation was controlled by processes related to microbial activity. At this stage it is not known whether this precipitation process took place in truly marine pore waters or in pore water of a modified composition. Future geochemical data are needed to better constrain the composition of the fluids from which micrite 2 precipitated and the conditions under which these bacteria lived.

ACKNOWLEDGMENTS

The author thanks ODP for providing the samples for this study and acknowledges the financial support of the Swiss National Science Foundation to participate in Leg 165. The analytical support of Alicia Thompson at the Center for Electron Microscopy at the University of Southern California, is gratefully acknowledged. The author acknowledges the accurate reviews by Daniel Bernoulli, Evan Franseen, and Mark Leckie.

REFERENCES

Bernoulli, D., Garrison, R.E., and McKenzie, J., 1978. Petrology, isotope geochemistry, and origin of dolomite and limestone associated with basaltic breccia, Hole 373A, Tyrrhenian Basin. *In* Hsu, K., Montadert, L., et al., *Init. Repts. DSDP,* 42 (Pt. 1): Washington (U.S. Govt. Printing Office), 541–558.

Bernoulli, D., and Weissert, H., 1985. Sedimentary fabrics in Alpine ophicalcites, South Pennine Arosa Zone, Switzerland. *Geology,* 13:755–758.

Boehlke, J.H., Honnorez, J., and Honnorez-Guerstein, J., 1980. Alteration of basalts from Site 396B, Deep Sea Drilling Project: petrographic and Mineralogical Studies. *Contrib. Mineral. Petrol.,* 73:341–364.

Chafetz, H.S., and Buczynski, C., 1992. Bacterially induced lithification of microbial mats. *Palaios*, 7:277–293.

Easton, A.J., Joslin, I.E., Kempe, D.R.C., and Hannock, J.M., 1982. Metasomatic alteration of pelagic ooze on spreading ocean ridges. *Mar. Geol.*, 48:M1–M6.

Folk, R.L., 1962. Practical petrographical classification of limestones. *AAPG Mem.,* 1:108–121.

Folk, R.L., and McBride, E.F., 1976. Possible pedogenic origin of Ligurian ophicalcite: a Mesozoic calichified serpentinite. *Geology,* 4:327–332.

Monty, C.L.V., 1995. The rise and nature of carbonate mud-mounds: an introductory actualistic approach. *In* Monty, C.L.V., Bosence, D.W.J., Bridges, P.H., and Pratt, B.R. (Eds.), *Carbonate Mud-mounds, Their Origin and Evolution.* Spec. Publ. Int. Assoc. Sedimentol., 23:11–48.

Morita, R.Y., 1980. Calcite precipitation by marine bacteria. *Geomicrobiol. J.*, 2:63–82.

Novitski, J.A., 1981. Calcium carbonate precipitation by marine bacteria. *Geomicrobiol. J.*, 2:375–388.

Sigurdsson, H., Leckie, R.M., Acton, G.D., et al., 1997. *Proc. ODP, Init. Repts.,* 165: College Station, TX (Ocean Drilling Program).

Staudigel, H., Gillis, K., and Duncan, R., 1986. K/Ar and Rb/Sr ages of celadonites from the Troodos ophiolite, Cyprus. *Geology,* 14:72–75.

Date of initial receipt: 23 June 1998
Date of acceptance: 19 January 1999
Ms 165SR-015

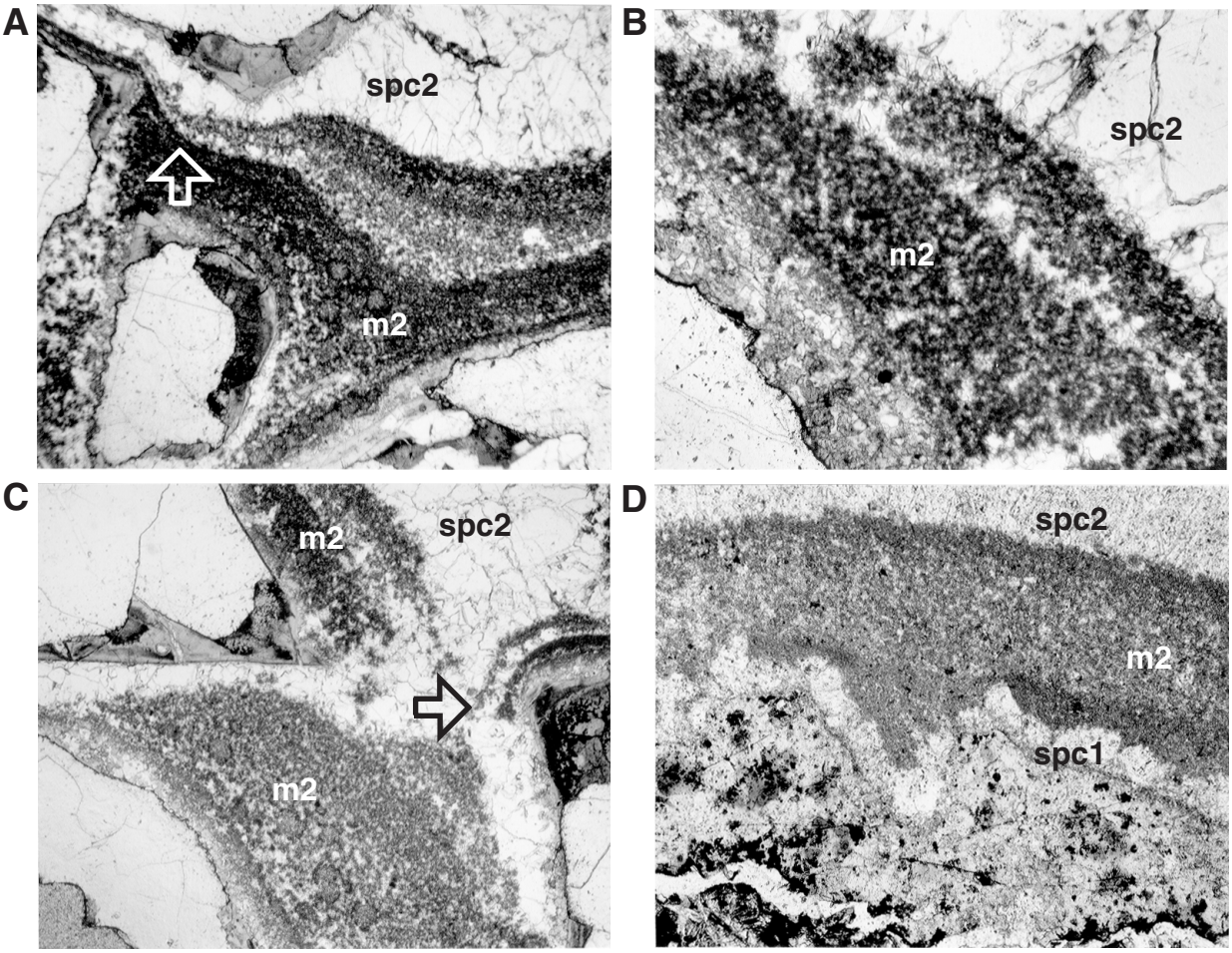

Figure 5. Optical microphotographs. **A.** Overview of laminated micrite 2 (m2) and sparry calcite 2 (spc2). Note how it occurs preferentially in geopetal orientation at the bottom of cavities and how laminae surfaces curve to mantle the substrate. The arrow indicates the contact between two major laminae characterized by an undulating topography (2.5×; interval 165-1001A-54R-1, 72–74 cm). **B.** Micritic lumps or "pseudopeloids" within two laminae of micrite 2 (m2), postdated by sparry calcite 2 (spc2) (6.3×; interval 165-1001A-54R-1, 72–74 cm). **C.** Arrow points to laminated remnant of micrite 2, which possibly underwent a phase of dissolution (2.5×; interval 165-1001A-54R-1, 72–74 cm). **D.** Sparry calcite 1 (spc1) is overlain by micrite 2 (m2) (6.3×; interval 165-1001A-54R-2, 87–90 cm), overlain in turn by sparry calcite 2 (spc2).

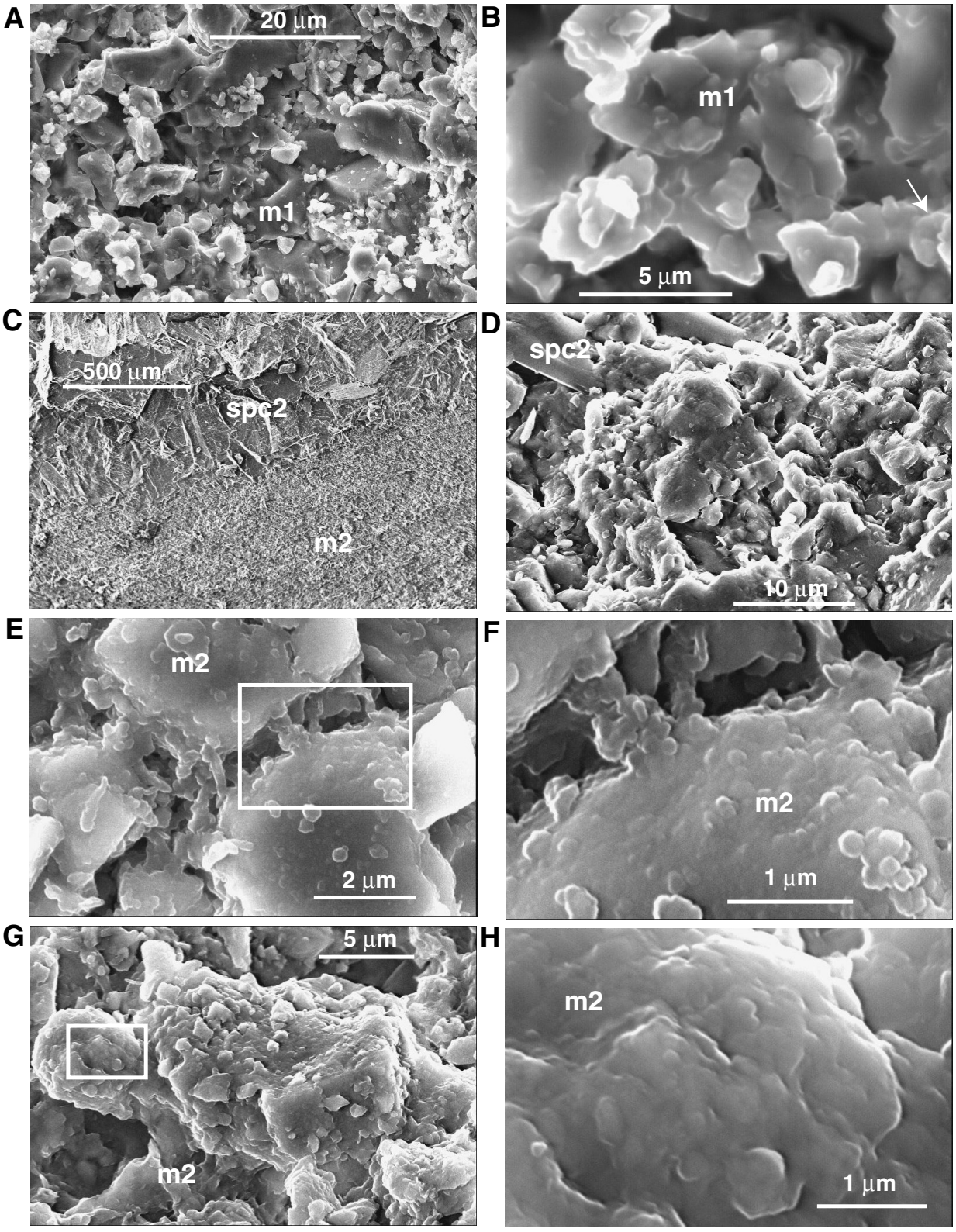

Figure 6. SEM photomicrographs. **A.** General aspect of micrite 1 (m1). Note the smooth surfaces of the crystals (interval 165-1001A-54R-5, 13–18 cm; see Fig. 3A). **B.** Close-up image of micrite 1 where it is possible to recognize the remnants of nannofossils (arrow) now almost entirely obliterated by recrystallization (interval 165-1001A-54R-5, 13–18 cm). **C.** Contact between micrite 2 (m2) and sparry calcite 2 (spc2) (interval 165-1001A-54R-1, 72–74 cm). **D.** Close-up of C, showing the detailed relationships between micrite 2 and sparry calcite 2 (spc2). Note the difference in appearance between micrite 1 as shown in A, and micrite 2 shown here. The crystals forming micrite 2 here are anhedral and their surfaces have a blobby appearance supporting microbial influence (interval 165-1001A-54R-1, 72–74 cm). **E.** View of micrite 2, made of euhedral to subhedral crystals with a blobby surface. The white rectangle indicates the field of view of image F (interval 165-1001A-54R-1, 72–74 cm). **F.** Detailed view of image E showing bridges between grains supporting microbial influence (interval 165-1001A-54R-1, 72–74 cm). **G.** The white rectangle indicates the field of view of image H (interval 165-1001A-54R-4, 67–72 cm). **H.** Blobby crystal surface forming a cauliflower structure supporting microbial influence (interval 165-1001A-54R-4, 67–72 cm).